J. Fluid Mech. (1994), *vol.* 264, *pp.* 81–106

Scale-dependent merging of baroclinic vortices

By J. VERRON AND S. VALCKE

URA 1509 CNRS, Institut de Mécanique de Grenoble, BP 53X, 38041 Grenoble Cédex, France

(Received 26 February 1993 and in revised form 22 September 1993)

The influence of stratification on the merging of like-sign vortices of equal intensity and shape is investigated by numerical simulations in a quasi-geostrophic, two-layer stratified model. Two different types of vortices are considered: vortices defined as circular patches of uniform *potential* vorticity in the upper layer but no PV anomaly in the lower layer (referred to as PVI vortices), and vortices defined as circular patches of uniform *relative* vorticity in the upper layer but no motion in the lower layer (referred to as RVI vortices). In particular, it is found that, in the RVI case, the merging behaviour depends strongly on the magnitude of the stratification (i.e. the ratio of internal Rossby radius and vortex radius). The critical point here appears to be whether or not the initial eddies have a deep flow signature in terms of PV.

The specific phenomenon of scale-dependent merging observed is interpreted in terms of the competitive effects of hetonic interaction and vortex shape. In the case of weaker stratification, the baroclinic structure of the eddies can be seen as dominated by a mechanism of hetonic interaction in which bottom flow appears to counteract the tendency of surface eddies to merge. In the case of larger stratification, the eddy interaction mechanism is shown to be barotropically dominated, although interface deformation still determines the actual eddy vorticity profile during the initialization stage. Repulsion (hetonic) effect therefore oppose attraction (barotropic shape) effects in a competitive process dependent on the relationship between the original eddy lengthscale and the first internal Rossby radius.

A concluding discussion considers the implications of such analysis for real situations, in the ocean or in the laboratory.

1. Introduction

Vortex merger is seen as a prototype mechanism for the evolution of two-dimensional turbulence which gives rise to long-lived, intense coherent vortices (Basdevant *et al.* 1981; McWilliams 1984). The merging process has received considerable attention from experimentalists as well as through theoretical and numerical investigations (Brown & Roshko 1974; Winant & Browand 1974; Zabusky, Hughes & Roberts 1979; Overman & Zabusky 1982; Melander, Zabusky & McWilliams 1988). It is not certain, however, that the highly idealized problem of the interaction of two like-sign vortices of equal intensity and shape is statistically significant in the evolution of such turbulence (Dritschel & Waugh 1992). Real processes are likely to be much more complicated, involving complex interactions of intricate vorticity structures. It is, however, quite clear that a considerable understanding of vortex dynamics has been gained from this simple, somewhat academic, configuration and that it can still be of considerable use (see, for example, the review paper by Hopfinger & van Heijst 1994).

The case of rotating stratified fluid is even more complicated and, as yet, little is known and *a fortiori* understood. New concepts such as 'alignment' or 'attachment',

which have been addressed recently by Polvani, Zabusky & Flierl (1989), McWilliams (1989) and Polvani (1991), must be added as scenarios for eddy interactions. Speculation on the dynamical importance of coherent vortices in geophysical flows, such as the Gulf Stream rings or the Aghulas current eddies, or lenses of Mediterranean water (meddies), also provide considerable motivation for this type of study. Single eddies generated in the Aghulas current, for example, are thought to convey heat at a rate which is a significant fraction of the meridional transfer of heat through the whole Atlantic (Gordon & Haxby, 1990).

The quasi-geostrophic two-layer model that was used in early investigations (Gryanik 1983; Hogg & Stommel 1985*a*; Griffiths & Hopfinger 1987; Polvani *et al.* 1989; Verron, Hopfinger & McWilliams 1990) is one of the simplest models of baroclinic eddy interaction which possesses all the dynamical ingredients for representing vortex interaction in a rotating stratified flow. In their laboratory experiments, Griffiths & Hopfinger (1987) found a marked effect of stratification on vortex merging, using a rotating tank containing two layers of different density but of equal depth. At that time, they suggested that the vortices created in their experiments could be modelled as circular patches of uniform potential vorticity in the upper layer (PVI vortices) but no potential vorticity anomaly in the bottom layer. However, Polvani *et al.* (1989) performed numerical computations with contour dynamics on the merging of PVI vortices and found no effect of the stratification when the two layers were of equal depth. The problem was reconsidered by Verron *et al.* (1990) who showed the importance of initial conditions on baroclinic vortex merging. In particular, they studied the merging of vortices defined as circular patches of uniform relative vorticity (RVI vortices) but no motion in the bottom layer. In that case, they found that the merging was strongly scale-dependent, i.e. that it was greatly influenced by the magnitude of the stratification, namely the ratio of internal Rossby radius and vortices radius.

The objective of the present study continue the preliminary work of Verron *et al.* (1990) and to explore further several unanswered questions: What are the consequences of the various ways of initializing our vortices on their vertical and horizontal structure? How can we interpret the scale-dependent effect of the stratification on the merging process observed in our simulations? What can we deduce from this interpretation to explain the merging behaviour of the laboratory vortices? On the basis of physical observations, what can we say about the applicability of our results to real eddies? What are the possible consequences of this scale dependency? While we give only a partial or speculative discussion of the last three points, the core of this paper treats and answers in great detail the first two questions.

The present paper is organized as follows. In §2, after an introduction to the quasi-geostrophic model to be used, the numerical results are presented on the various merging situations and associated initial conditions. Section 3 provides an interpretation of the enhanced tendency to merge for a selective range of scales in RVI conditions. Section 4 discusses some aspects of real (oceanic and laboratory) vortices and modelled eddies with regard to the problem in question.

2. Merging

2.1. *Quasi-geostrophic model*

A standard model for the two-layer vortex dynamics is provided by the following quasi-geostrophic set of equations for the potential vorticity Q_i (Pedlosky 1979):

$$\frac{DQ_1}{Dt} = V_1, \tag{1a}$$

$$\frac{DQ_2}{Dt} = V_2, \tag{1b}$$

where

$$\frac{DQ_i}{Dt} = \frac{\partial Q_i}{\partial t} + J(\psi_i, Q_i),$$

$$Q_1 = \omega_1 + f_0 + \frac{f_0^2}{g' H_1}(\psi_2 - \psi_1), \tag{2a}$$

$$Q_2 = \omega_2 + f_0 - \frac{f_0^2}{g' H_2}(\psi_2 - \psi_1), \tag{2b}$$

and ψ_i are the streamfunctions from which the two components of the horizontal velocity, written as $u = -\partial\psi/\partial y$, $v = \partial\psi/\partial x$, and the relative vorticities, $\omega_i = \nabla^2\psi_i$, can be calculated. The Jacobian J is written as

$$J(\psi, Q) = \frac{\partial\psi}{\partial y}\frac{\partial Q}{\partial x} - \frac{\partial\psi}{\partial x}\frac{\partial Q}{\partial y}.$$

The planetary vorticity associated with background rotation is assumed to be a constant f_0(the f-plane approximation). It is clear that this constant term has no effect on the dynamical equations because of the operator D/Dt. It is therefore dropped in subsequent equations for the sake of simplicity. The last term in the potential vorticity expressions, Q_i, represents the vortex stretching term coupling the two layers. V_i represents a dissipative term, the form of which is discussed in more detail below. The subscript 1 indicates the upper layer, 2 the bottom layer. g' measures the density jump, $\Delta\rho$, between the two layer such that

$$g' = g\frac{\Delta\rho}{\rho}$$

where ρ is the reference mean density. The limitations of this model are those of the quasi-geostrophic approximation. In defining $H = H_1 + H_2$, the total fluid depth, L, the horizontal scale, and U, the horizontal velocity scale, the Rossby number $\epsilon = U/f_0 L$ must be small in relation to 1 (geostrophy), and the aspect ratio H/L also much smaller than 1 (hydrostaticity). In addition, the density jump must be small compared with the basic stratification, $\Delta\rho \ll \rho$ (Boussinesq).

If we assume that dissipation is negligible, the flow will be simply governed by the Lagrangian conservation of potential vorticity in each layer:

$$\frac{DQ_1}{Dt} = \frac{D}{Dt}\left[\omega_1 + \frac{H_2}{H_1 + H_2}\lambda^{-2}(\psi_2 - \psi_1)\right] = 0, \tag{3a}$$

$$\frac{DQ_2}{Dt} = \frac{D}{Dt}\left[\omega_2 - \frac{H_1}{H_1 + H_2}\lambda^{-2}(\psi_2 - \psi_1)\right] = 0, \tag{3b}$$

with Q_1 and Q_2 subject to some initial conditions expressed by the potential vorticity

fields Q_{10} and Q_{20} in the upper and lower layers respectively. The internal Rossby radius of deformation for the system is written as

$$\lambda = \left[\frac{g' H_1 H_2}{f_0^2 (H_1 + H_2)}\right]^{\frac{1}{2}}. \tag{4}$$

If we assume $H_1 = H_2 = H$, λ reduces to

$$\lambda = \frac{(g' H)^{\frac{1}{2}}}{\sqrt{2} f_0} \tag{5}$$

and the set of equations is written

$$\frac{\mathrm{D}Q_1}{\mathrm{D}t} = \frac{\mathrm{D}}{\mathrm{D}t}[\omega_1 + \tfrac{1}{2}\lambda^{-2}(\psi_2 - \psi_1)] = 0, \tag{6a}$$

$$\frac{\mathrm{D}Q_2}{\mathrm{D}t} = \frac{\mathrm{D}}{\mathrm{D}t}[\omega_2 - \tfrac{1}{2}\lambda^{-2}(\psi_2 - \psi_1)] = 0. \tag{6b}$$

In any case, the interface deviation η is written as

$$\eta = \frac{f_0}{g'}(\psi_2 - \psi_1).$$

None of our simulations has been strictly potential-vorticity conserving, because of subgrid-scale parameterization. For simplicity, in the rest of this paper we will sometimes disregard this 'viscosity' effect and refer to potential vorticity conservation, in which case the simplified inviscid framework as given by (6) will apply.

Note that in a quasi-geostrophic model no difference many be observed between cyclones and anticyclones. In laboratory experiments carried out in rotating tanks, like those used by Griffiths & Hopfinger (1987), it was observed that Ekman pumping causes cyclonic vortices to diffuse more rapidly than anticyclonic vortices. In addition, Carnevale *et al.* (1991) showed that the effect of a parabolic free surface in the experiments is to make the cyclones/anticyclones travel along inward/outward spiral trajectories, thereby promoting cyclone merger and inhibiting anticyclone merger to some degree.

Barotropic limiting conditions can be met in two ways. For large values of λ, stratification is pronounced and in the limiting case, $\lambda \to \infty$, layers may act independently. When motion is initiated only in the upper layer, one is reduced to studying only this homogeneous upper layer. For small values of λ, stratification is modest and layers are very closely coupled together. At the limit $\lambda \to 0$, they are perfectly coupled and we are reduced to studying the motion of one equivalent layer of depth $H_1 + H_2$. However, the strict limit, $\lambda = 0$, is inconsistent with having a motion initiated only in the upper layer. Moreover, for small values of λ, baroclinic instabilities may develop together with merging.

The numerical code solves the vorticity equations written for the barotropic mode and the first baroclinic mode, respectively, as $\psi_{BT} = 1/2(\psi_1 + \psi_2)$ and $\psi_{BC} = 1/2(\psi_1 - \psi_2)$ when $H_1 = H_2$, using classical finite-difference schemes. The Helmholtz equations resulting from the discretization in time are solved with a pseudospectral algorithm. In the present case, it is assumed that dissipation includes no bottom friction. However, the terms V_i of equations (1*a*) and (1*b*) are needed to dissipate the

enstrophy which tends to accumulate at the small scales not resolved by the model. These terms can take the form of lateral dissipation of the Laplacian type, $V_i = A_l \nabla^2 \omega_i$, or the form of a high-order viscosity term ('biharmonic' friction), $V_i = -A_4 \nabla^4 \omega_i$. The latter, which was chosen here, has a stronger small-scale selectivity with regard to dissipation than the former; the high-order biharmonic viscosity term is therefore more efficient at damping the small scales without appreciably affecting the larger scales of interest (Holland 1978). As our aim is to simulate a nearly inviscid flow, the coefficient A_4 is chosen as small as possible without allowing spurious numerical noise to develop at the grid scale of the model.

Studying interaction of baroclinic vortices clearly requires some assumptions on the structure of the initial baroclinic vortices under consideration. *Verron et al.* (1990) have shown that the question of initial conditions has consequences for merging which are by no means trivial. The following paragraphs present the results of the numerical simulations performed to explore the conditions for the merging of baroclinic vortices when the vortices are defined in the upper layer of a two-layer stratified fluid as equal patches of either potential vorticity or relative vorticity, or a mixture of both.

2.2. *Potential vorticity initialization*

If one considers the upper vortices as circular patches of pure uniform potential vorticity, i.e. having a profile of the Rankine type (designated R_a), the initial conditions for the set of equations (3) may be written as follows:

$$Q_{10} = \sum_{k=1,2} R_a^k, \tag{7a}$$

$$Q_{20} = 0. \tag{7b}$$

The summation $k = 1, 2$ on R_a^k indicates a pair of Rankine vortices. These vortices are of equal intensity, sign and radius R, and their initial distance is d. This provides us with the so-called Potential Vorticity Initialization (PVI).

In our numerical simulations, the Rankine vortex profile was approximated by the following expression:

$$R_a^k \approx \Omega[1 - 0.5(\tanh X + 1)],$$

where Ω is the maximum value of the potential vorticity in the core and $X = \mu(r/R - 1)$, with r the radial distance from the centre of the vortex k. The coefficient μ measures the relative thickness of the vorticity jump of such modified Rankine vortices. In our numerical simulations, the finite value of $\mu = 4$ was chosen to avoid the Gibb's instabilities that would appear for a pure Rankine vortex (which corresponds to $\mu \to \infty$). Other parameters for our numerical simulations were chosen, as far as possible, according to the Griffiths & Hopfinger experiments: $L = 1$ m, $R = 0.04$ m, $H = 0.2$ m, $f_0 = 2\ \mathrm{s}^{-1}$. For numerical simplicity, the domain is a square of dimensions $L \times L$, instead of a circular tank. The vortex amplitude Ω is generally taken as $\Omega = 2\ \mathrm{s}^{-1}$. The stratification jump is varied in order to vary the corresponding value of λ in the range of interest.

Figure 1 shows the initial upper- and lower-layer potential vorticity, relative vorticity, streamfunction and azimuthal velocity for this type of initialization, for different background stratification values expressed by the internal Rossby radius of deformation, λ, scaled by R, the radius of the vortex core. By assumption, the potential vorticity profiles are identical for all degrees of stratification. Relatively small differences are observed for the relative vorticity profiles in the upper layer, except that 'shielding', i.e. an annulus of opposite-sign vorticity around the core, becomes

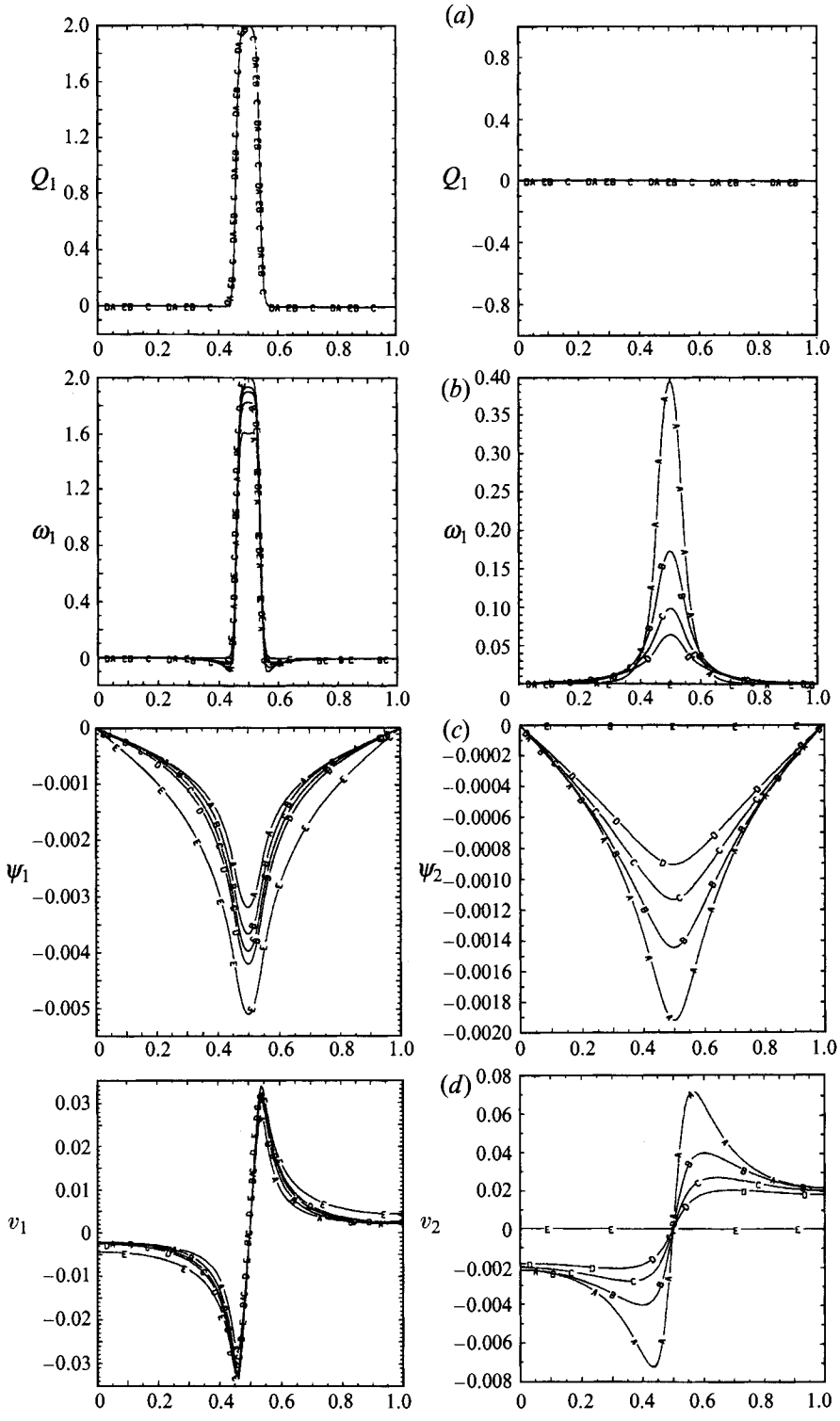

FIGURE 1. Potential Vorticity Initialization of a single vortex: cross-sections of (*a*) potential vorticity (s^{-1}), (*b*) relative vorticity (s^{-1}), (*c*) streamfunction ($m^2\ s^{-1}$), (*d*) azimuthal velocity ($m^2\ s^{-1}$) at the centre of the domain for the upper-layer (1) and the lower-layer (2). The abscissa of the plots represents the horizontal dimension of the domain (m). The different curves are for various values of the Rossby radius λ/R = A, 1; B, 2; C, 3; D, 4; E, ∞.

increasingly pronounced as λ/R decreases. The lower-layer relative vorticity increases as λ/R decreases. It is also interesting to note that the initial azimuthal velocity profile varies with stratification, especially in the lower layer.

Despite this dependence of initial velocities on stratification, the critical merger distance, d_c, which is the distance between the vortex centres below which the vortices merge and above which they do not merge, was found to be insensitive to stratification by Polvani *et al.* (1989) using the contour dynamics method with this type of initialization for pure Rankine profiles. This result is also obtained with our model.

The concept of the critical merger distance is a useful and practical one which has been widely used in past studies, including recent studies by the present authors. But further consideration of viscous effects in our study led to the conclusion that this concept is sometimes misleading and/or inapplicable when characterizing the merging process. Indeed, in any viscous situation, the critical merger distance is subject to consideration of the time factor. Under the effect of viscosity, all vortices will eventually merge whatever the amplitude of their initial separation, d/R. This will normally occur at viscous timescales that are large compared with the advective timescales that are of interest here. Note that the influence of viscosity on merging has already been discussed by Melander *et al.* (1988). Taking into account the temporal dimension of merger evolution, the critical distance could therefore be understood as the boundary between merging and no merging on a convective timescale. However, we have found that in practice this distinction is difficult to make.

For example, let us look at figure 2 which shows the merger time t_c, non-dimensionalized by $T = 2\pi/\Omega$ (turnover period for the vortices) for the barotropic case $\lambda/R \to \infty$. This time t_c/T is expressed as a function of d/R for different values of the non-dimensional numerical viscosity $A_4^* = A_4/\Omega R^4$. (Merging being almost insensitive to stratification in the PVI case, the curves would be similar for any value of λ/R.) For d/R up to about 3.4, viscosity has practically no influence on t_c/T: these mergers can be seen as 'convective'. For $d/R \geqslant 3.6$, the simulations show that t_c/T increases drastically, especially for the smallest viscosities, but it is difficult to say that an asymptotic behaviour is observable. Two regimes may be identified: a convective merger regime occurring on a convective timescale and a viscous merger regime occurring on a viscous timescale. In principle, the critical distance should be determined as the boundary between these two regimes. But, as can be seen on the curves in figure 2, even for the smallest viscosity it is rather arbitrary to decide precisely where this limit should be. For this reason, we have decided not to base our view of merging on the critical distance concept but rather to consider the time t_c/T required for merging as the relevant vortex interaction factor.

In any event, the non-dimensional critical merger distance in our case (d_c/R somewhere between 3.4 and 3.8) would have been rather different from the 3.2 or 3.3 predicted for pure Rankine vortices from theoretical and numerical barotropic calculations (Zabusky *et al.* 1979; Overman & Zabusky 1982; Melander *et al.* 1988; Waugh 1992). This difference is due to the specific shape of the modified Rankine profile chosen. Indeed, the departure from the pure Rankine profile ($\mu = 4$ instead of ∞) is sufficient to infer a noticeable variation in the merging process. The convergence towards a value of d_c/R closer to 3.3 should be obtained for increased values of μ, but consistent numerical computations then would require increased resolution and involve higher computational costs. Note that, in their laboratory experiments, Griffiths & Hopfinger (1987) also found a critical distance of $d_c/R = 3.3 \pm 0.2$ for the barotropic merger of anticyclonic vortices (as mentioned previously, viscous, free-surface and other ageostrophic effects make the case of cyclones specific) whose profiles

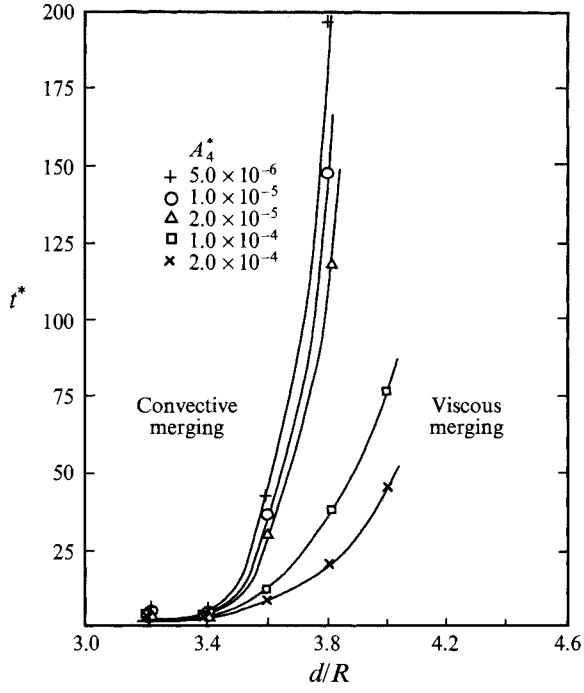

FIGURE 2. Merger time t_c/T as a function of d/R for different values of the viscosity A_4^* for the barotropic case.

probably did not strictly fall within the Rankine representation. Their findings regarding the value of d_c/R (≈ 3.3) may be related more to specific experimental conditions than the strict satisfaction of the Rankine theoretical framework.

Figure 3 presents a time sequence of the potential vorticity field showing the computed development of interaction between the vortices leading to merging. Note that this sequence has all the familiar features of the evolution of relative vorticity during barotropic merger (see, for example, figure 1 of Melander *et al.* 1988). The vortices approach each other as they rotate about their mutual centre of vorticity, then merging *per se* takes place and finally axisymmetrization is reached through filamentation. We observed that this evolution is typical of all mergers in the PVI case, whatever the stratification. The only influence of stratification seems to be that for greater λ/R axisymmetrization is slightly faster. We cannot strictly say that stratification has no influence on vortex interaction in the PVI case, but its influence does appear very limited and was not significant with regard to merging characteristics such as merger time or critical distance.

2.3. *Relative vorticity initialization*

If we now assume that the bottom layer is at rest and that the initial vortices are defined as two Rankine profiles of relative vorticity in the upper layer, the initial flow fields will be $\psi_{20} = 0$ and $\psi_{10} = \psi_a$, given by

$$\nabla^2 \psi_a = \sum_{k=1,2} R_a^k.$$

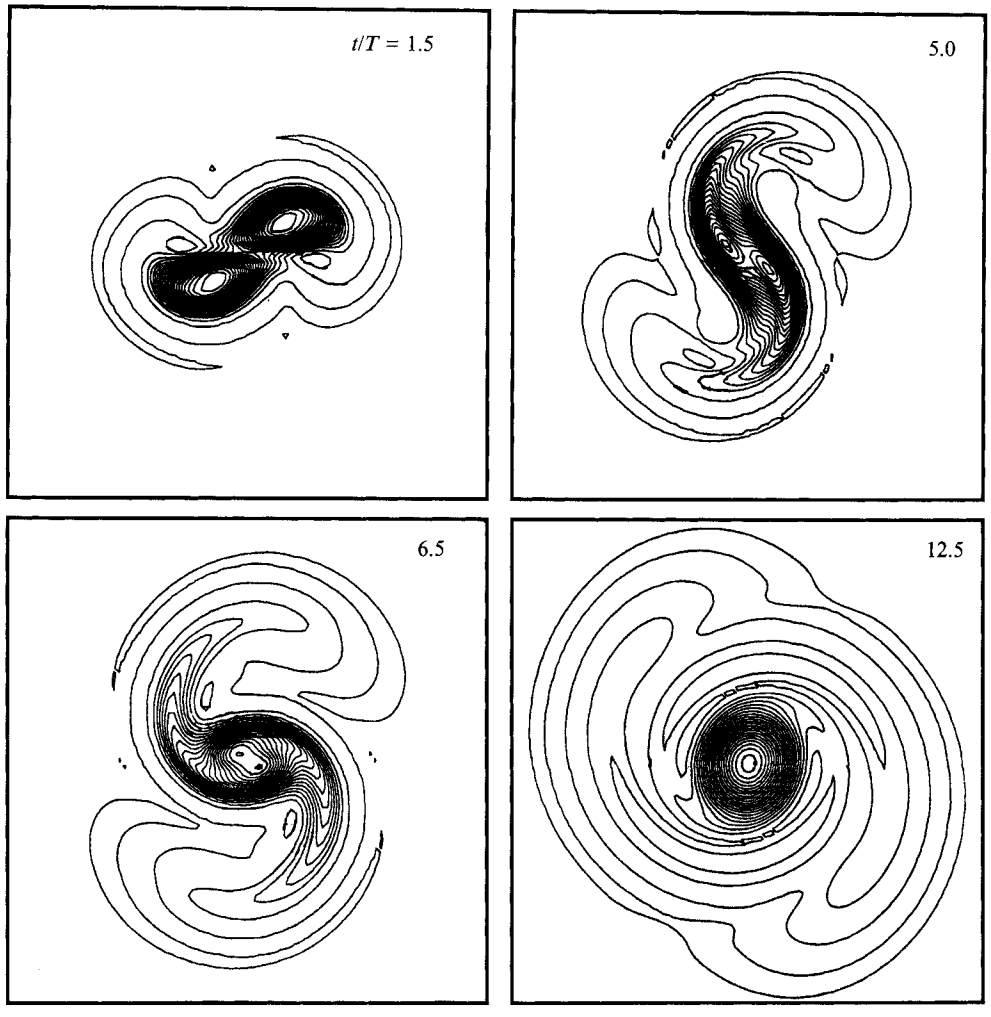

FIGURE 3. A merging sequence in the PVI case for $\lambda/R = 1$ and $d/R = 3.1$: potential vorticity field of the upper layer at $t/T = 1.5$, 5.0, 6.5, 12.5.

Consequently, the initial potential vorticity in the two layers is

$$Q_{10} = \sum_{k=1,2} R_a^k - \tfrac{1}{2}\lambda^{-2}\psi_a, \tag{8a}$$

$$Q_{20} = +\tfrac{1}{2}\lambda^{-2}\psi_a \tag{8b}$$

This is the Relative Vorticity Initialization (RVI) as introduced by Verron *et al.* (1990).

Figure 4 shows the various initial fields associated with this type of initial condition. In this case, by assumption, the initial relative vorticity profiles, and consequently the initial streamfunction and velocity fields, are invariant with respect to stratification. In particular, the vertical shear associated with the baroclinic mode is constant. However, the initial potential vorticity profiles are dependent on background stratification expressed by λ/R, where R is now the radius of the vortex core in relative vorticity. The upper-layer potential vorticity has a similar modified Rankine profile for large λ/R but it increases progressively as λ/R diminishes, acquiring an increasingly pronounced 'skirt' shape. This is a direct effect of the vorticity stretching term, $\frac{1}{2}\lambda^{-2}\psi_a$, coupling the

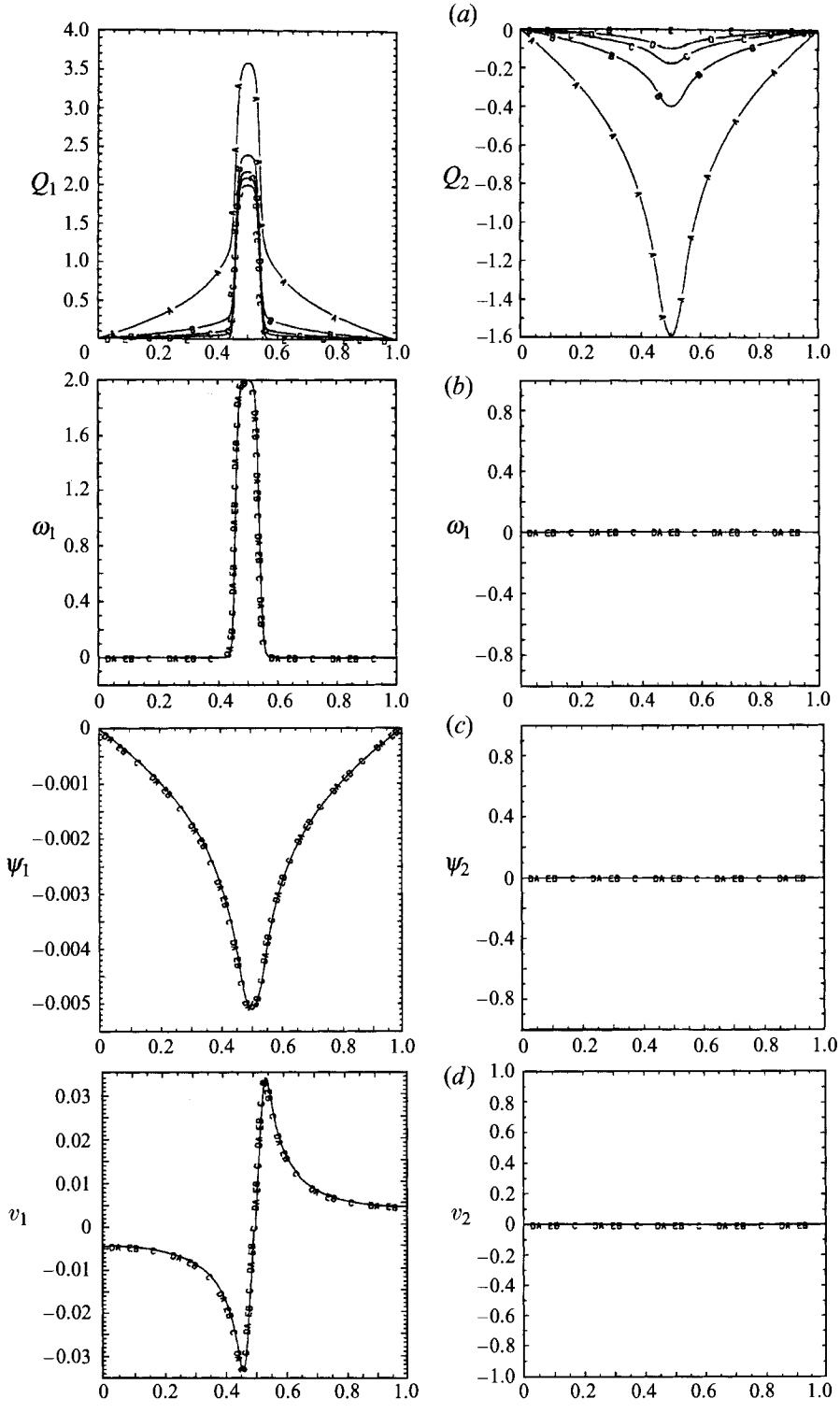

FIGURE 4. As figure 1 but for the Relative Vorticity Initialization of a single vortex.

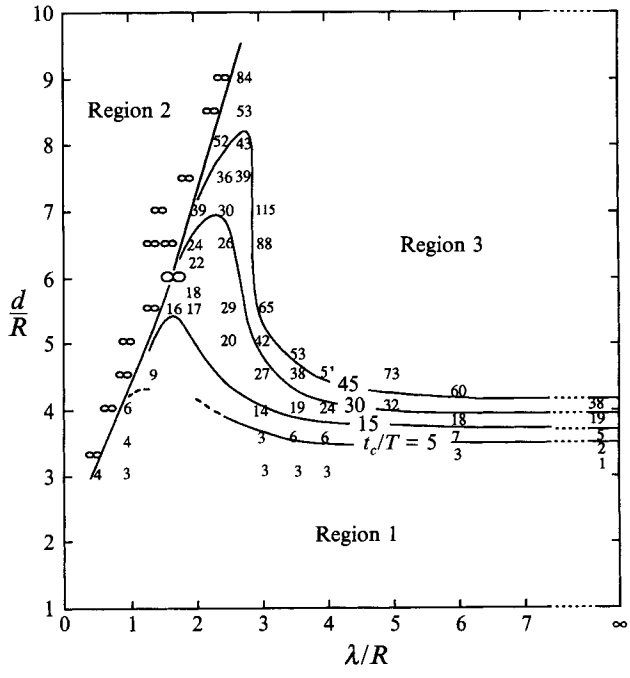

FIGURE 5. Merger time t_c/T as a function of d/R and λ/R for the RVI simulations with $A_4^* = 1 \times 10^{-4}$. In Region 1, merging occurs rapidly on a convective timescale; in Region 2, the vortices diverge from one another and never merge; in Region 3, viscous merging eventually occurs on a much longer viscous timescale. The isocurves for $t_c/T = 5$, 15, 30, 45 and ∞ are shown.

two layers. In the lower layer, this term is of opposite signs and creates, in potential vorticity, a negative skirt-shaped vortex associated with each vortex defined in the upper layer. The main difference in relation to PVI is that now the initial potential vorticity profiles in both layers depend on stratification. The vortices have skirt shapes and for small values of λ/R the potential vorticity induced in the lower layer becomes comparable in intensity to the potential vorticity of the upper layer.

In the RVI case, merging was found to be strongly dependent on background stratification, as can be seen in figure 5. This shows the time t_c/T required for merging as a function of the initial distance d/R and of the stratification parameter λ/R. In figure 5, three regimes of vortex interaction may be roughly identified. Region 1 corresponds to where merging occurs. Under each isocurve of t_c/T, merging occurs in a time less than the corresponding value of t_c/T. The interesting point is that a marked peak subregion can be identified where merging occurs in much shorter times than would be the case in a barotropic situation. For example, for an initial distance d/R as large as 6.5, and when $\lambda/R \approx 2.5$, merging can be obtained after a time t_c/T of around only 26, while it would be at least 3 times longer for a larger stratification parameter λ/R such as 3.0. Merging is therefore very much favoured for a restricted range of λ/R, between around 1.5 and 3. In Region 2, on the other hand, the vortices do not merge and the distance separating them increases with time. The merger time, t_c/T, was therefore set at ∞. The region where merging is inhibited is well defined by a curve with a slope $d/\lambda \approx 2.5$. In Region 3, the vortices do not merge on a convective timescale. Merging will occur there over longer times, typical of the viscous timescales. For large λ/R, the merger times t_c/T become almost invariant with stratification and similar to their barotropic value. Figure 6 shows a parallel time sequence of the

potential vorticity in each layer for the three types of interaction observed, corresponding to the three regions mentioned above.

The possibility of presenting the results of figure 5 in terms of critical distance instead of merger time was considered. As discussed earlier, however, this was not found to be a very satisfactory quantitative approach because of the uncertainty in defining the limit between convective merging and viscous merging and thus of assigning a value to the critical distance. The viscous timescale problem was even more crucial than in the PVI situation, since large integration times were required to delimit the peak region.

The appearance of a peak in Region 1 and of inhibited merging in Region 2 is an important feature of vortex interaction in the RVI case. It is particularly interesting to note that, in the RVI case, although the various potential vorticity profiles are dependent on the Rossby radius, this is not the case for the initial velocity fields and they remain exactly the same for all stratification conditions. This does not prevent stratification from exerting a marked influence on the further evolution of flow.

2.4. *Mixed vorticity initialization*

Another type of initialization that may be considered, designated Mixed Vorticity Initialization (MVI), illustrates well merger sensitivity to initial conditions and, in several respects, is more compatible with what we know of Griffiths & Hopfinger's laboratory experiments, as will be discussed later. Let us assume the following initial potential vorticity in two layers:

$$Q_{10} = \sum_{k=1,2} R_a^k + \tfrac{1}{2}\lambda^{-2}(\psi_{20} - \psi_{10}), \tag{9a}$$

$$Q_{20} = 0. \tag{9b}$$

This corresponds to a situation with a relative vortex initialization in the upper layer (as in RVI) and uniform potential vorticity in the bottom layer (as in PVI). The initial streamfunction fields, ψ_{10} and ψ_{20}, are then obtained by solving the system

$$\nabla^2\psi_{10} = \sum_{k=1,2} R_a^k, \tag{10a}$$

$$\nabla^2\psi_{20} - \tfrac{1}{2}\lambda^{-2}\psi_{20} = -\tfrac{1}{2}\lambda^{-2}\psi_{10} = -\tfrac{1}{2}\lambda^{-2}\psi_a. \tag{10b}$$

Figure 7 shows the upper-layer potential vorticity profile of one vortex resulting from this type of initialization for different λ/R values. Globally, the potential vorticity profile becomes greater as λ/R decreases, as can be seen in figure 7(*a*). But it is interesting to note that for small values of λ/R the 'skirt' shape becomes progressively restricted to a region closer to the core of the vortex. This is well illustrated in figure 7(*b*) for values of λ/R decreasing from 2 to 1.

The merging behaviour for this case is shown in figure 8. As in the RVI case, stratification influences merging: an increased tendency to merge, less pronounced than in the RVI case but still noticeable, is observed for $0.5 < \lambda/R < 2.5$ approximately.

2.5. *The 'reduced gravity' case*

Note that another interesting approximation is the 'equivalent barotropic' situation or 'reduced gravity' case. This is the limiting case when the bottom layer is infinitely deep ($H_2 \to \infty$) which results in (3) becoming

$$\frac{\mathrm{D}Q_1}{\mathrm{D}t} = \frac{\mathrm{D}}{\mathrm{D}t}[\omega_1 - \lambda^{-2}\psi_1] = 0, \tag{11}$$

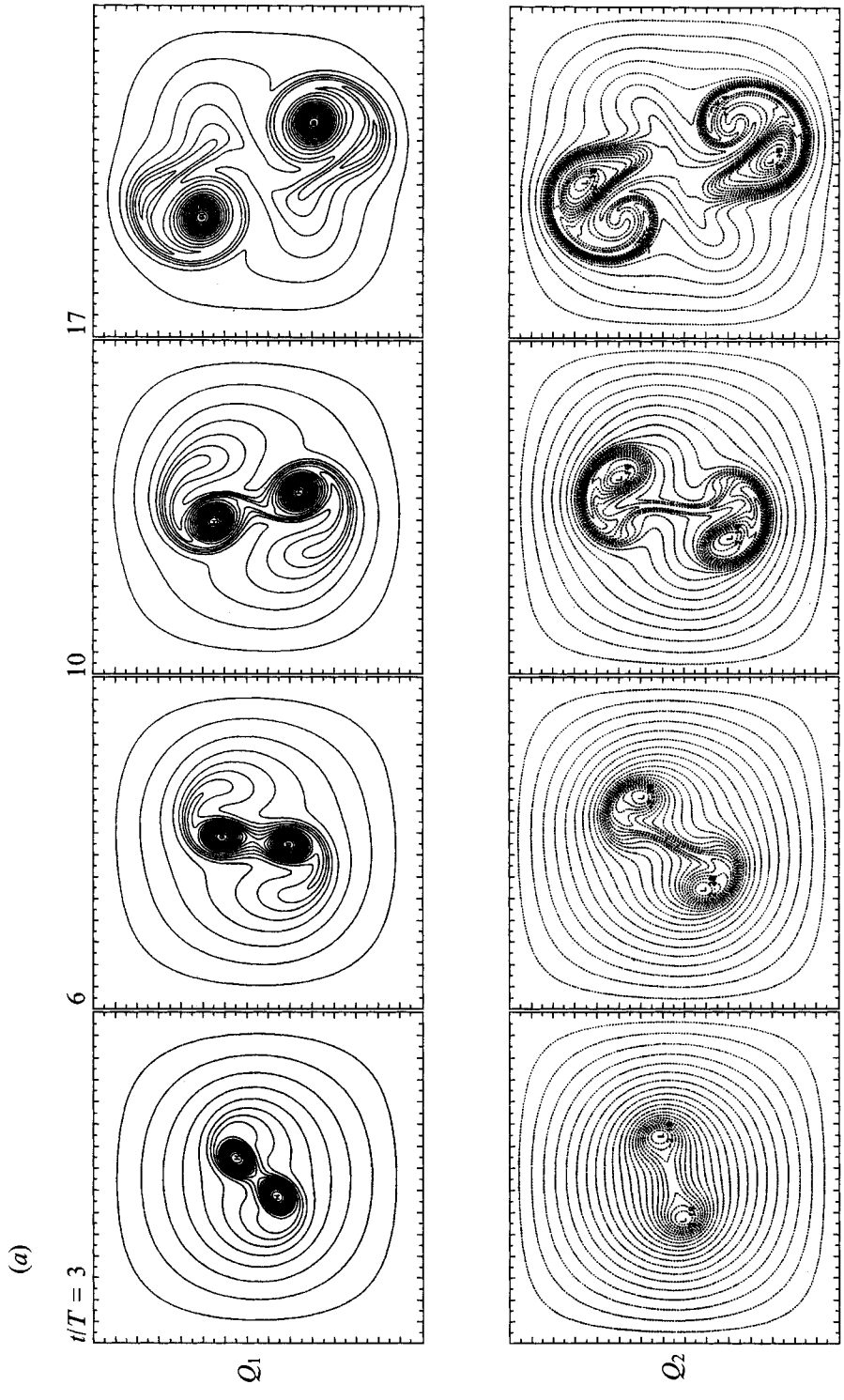

FIGURE 6(*a*). For caption see p. 95.

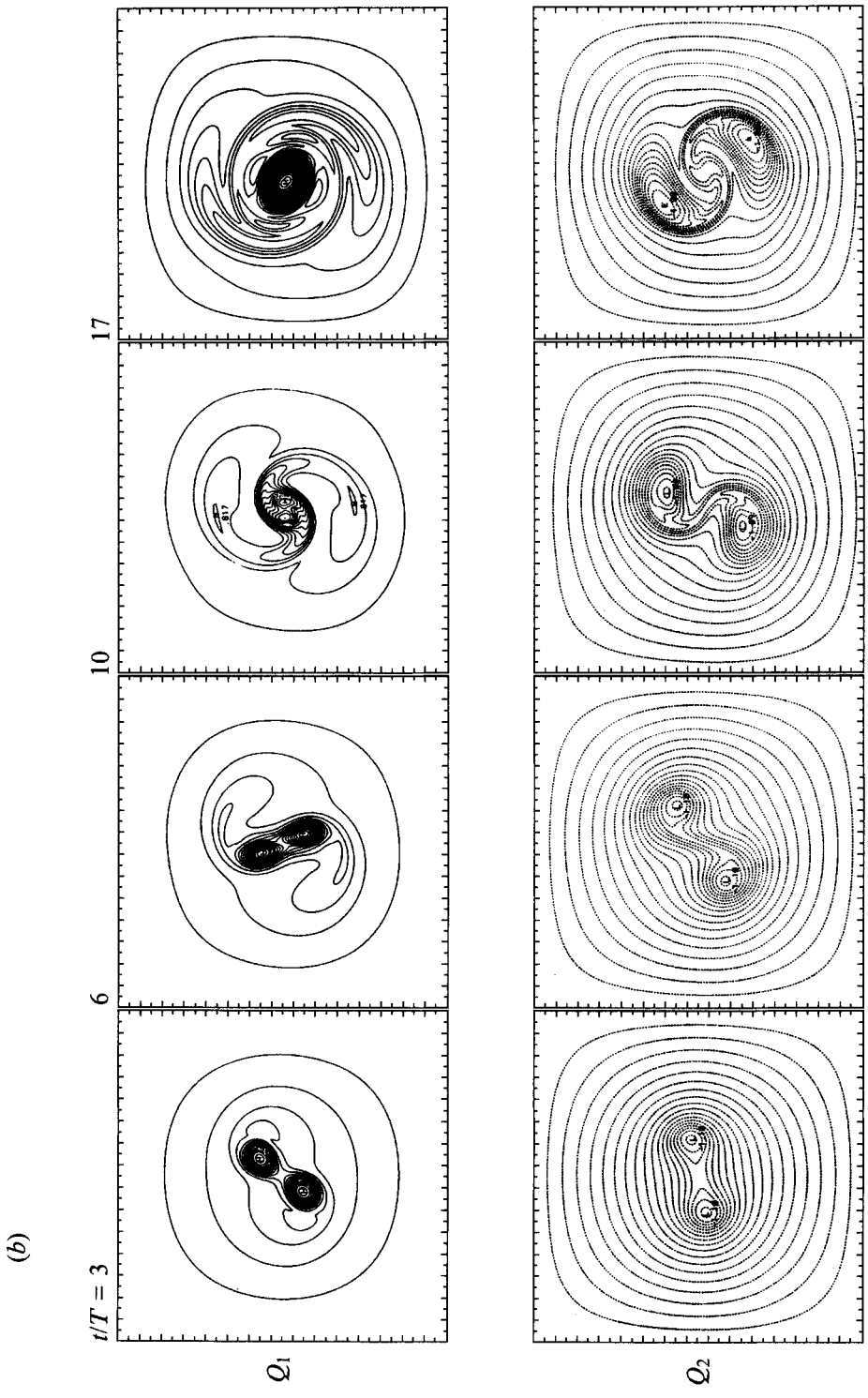
(b)
t/T = 3
6
10
17
Q1
Q2

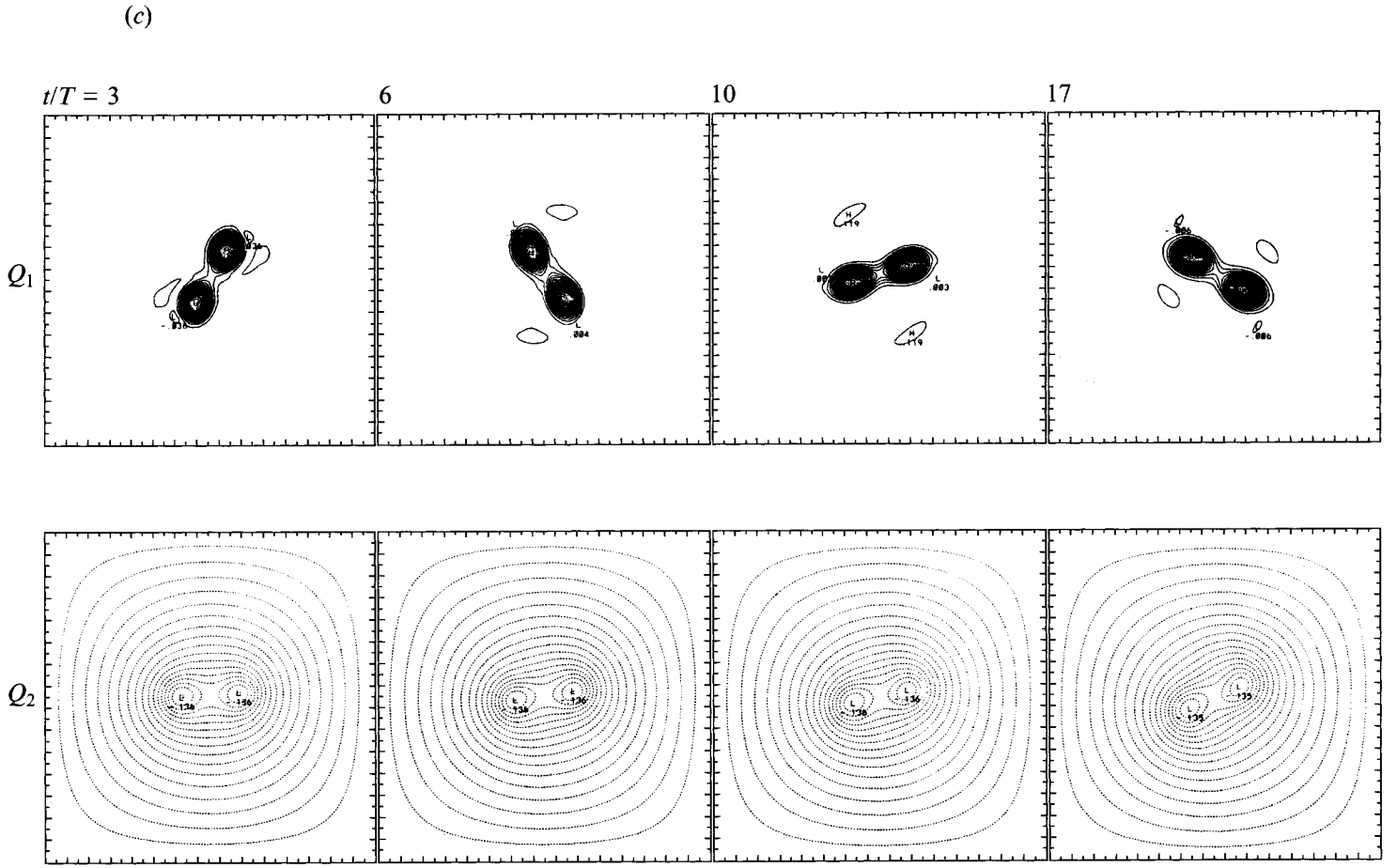

FIGURE 6. A parallel time sequence of the potential vorticity in the two layers for the three types of interaction observed: (*a*) $d/R = 4.5$, $\lambda/R = 1$: the vortices diverge from one another (Region 2); (*b*) $d/R = 4.5$, $\lambda/R = 1.41$: the upper-layer vortices merge (Region 1); (*c*) $d/R = 4.5$, $\lambda/R = 3.0$: the vortices do not merge on a convective timescale (Region 3).

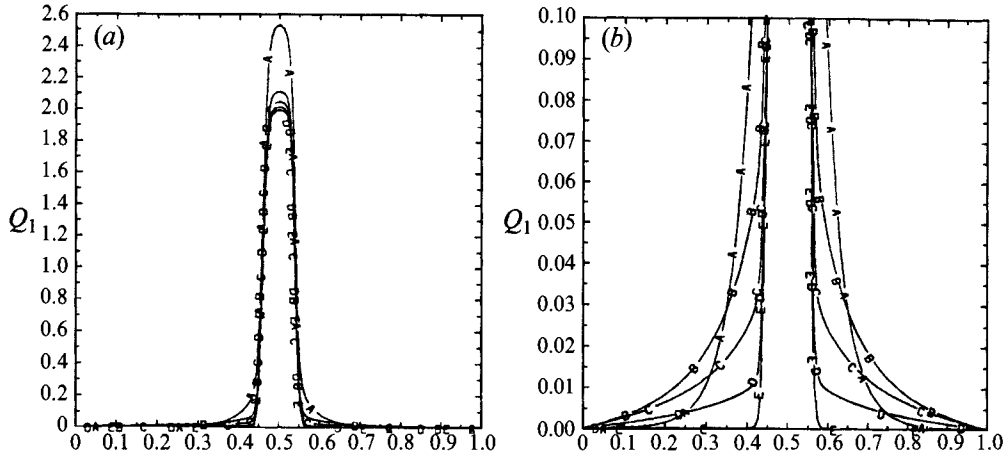

FIGURE 7. Mixed Vorticity Initialization of a single vortex: (*a*) cross-section and (*b*) close-up of the upper-layer potential vorticity (s^{-1}) at the centre of the domain. The abscissa of the plots represents the horizontal dimension of the domain (m). The different curves are for various values of the Rossby radius λ/R = A, 1; B, 2; C, 3; D, 4; E, ∞.

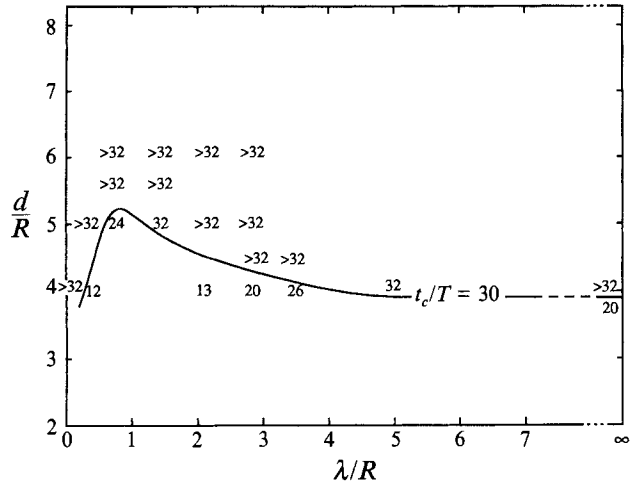

FIGURE 8. Merger time t_c/T as a function of d/R and λ/R for the MVI simulations with $A_4^* = 1 \times 10^{-4}$. The isocurve for $t_c/T = 30$ is shown.

in which λ is then written as

$$\lambda = \frac{(g'H_1)^{\frac{1}{2}}}{f_0}.$$

Here, an RVI way of writing the initial conditions is

$$Q_{10} = \sum_{k=1,2} R_a^k - \lambda^{-2}\psi_{10}, \tag{12}$$

still with $\nabla^2\psi_{10} = \sum_{k=1,2} R_a^k$.

The above problem can be referred to as the RVI reduced-gravity situation. Its PVI counterpart also exists and has been solved by Polvani *et al.* (1989). They found

that the critical distance d_c/R did not vary as a function of stratification except for $\lambda/R < 2$, for which a slight decrease in d_c/R was observed (their figure 14). The RVI case, as formulated by (11) and (12), seems to provide merging situations qualitatively of the same type as described in figure 5, except that merging is dramatically enhanced for smaller λ/R, even at very large initial distances d/R (McWilliams 1991, personal communication). In such a situation, computations become very delicate.

3. Attraction/repulsion effects

A fruitful approach to the further interpretation of the RVI situation was found by examining limiting dynamical situations with regard to the crucial role of baroclinicity and the effect of layer coupling. In this section of the paper, two opposite effects of stratification are identified for the RVI case and, based on this analysis a coherent explanation is proposed for the influence of stratification in the different types of initialization described above.

We begin by analysing the effects of varying the stratification of two extreme values of the non-dimensionalized internal Rossby radius λ/R in the RVI case. It will be shown that varying λ/R in strongly stratified regime has an opposite effect to that obtained in a weakly stratified regime. In the first case, a stronger attraction results between the upper-layer vortices, while in the second case there is a greater tendency for these vortices to diverge from each other.

3.1. *Barotropic shape effect*

The considerable influence of stratification on merging in the RVI case may at first appear surprising, as the initial velocity fields are independent of stratification (see figure 4). To understand the effect of stratification, one has to carefully consider the initial profiles of the dynamically conserved quantity, namely the potential vorticity.

Let us assume first that the dynamical effect of baroclinic coupling on the upper layer is negligible, i.e. the stretching term is small compared with the relative vorticity term:

$$\frac{\mathrm{D}}{\mathrm{D}t}[\tfrac{1}{2}\lambda^{-2}(\psi_2-\psi_1)] \ll \frac{\mathrm{D}\omega_1}{\mathrm{D}t}.$$

Equations (6) will reduce to

$$\frac{\mathrm{D}Q_1}{\mathrm{D}t} = \frac{\mathrm{D}\omega_1}{\mathrm{D}t} = 0,$$

$$\frac{\mathrm{D}Q_2}{\mathrm{D}t} = \frac{\mathrm{D}\omega_2}{\mathrm{D}t} = 0$$

still assuming the same initial conditions (8):

$$Q_{10} = \sum_{k=1,2} R_a^k - \tfrac{1}{2}\lambda^{-2}\psi_{10},$$

$$Q_{20} = +\tfrac{1}{2}\lambda^{-2}\psi_{10}.$$

Note that the term $\frac{1}{2}\lambda^{-2}\psi_{10}$, corresponding to the initial interface deformation, is kept in the initial definition of the vorticity profile in the two layers, but it is assumed to play no further role in the dynamics. In this case, layer equations are indeed uncoupled and the merging problem for the upper layer reduces to a purely barotropic problem in which the initial profile of vorticity is subject to the above initial conditions. The

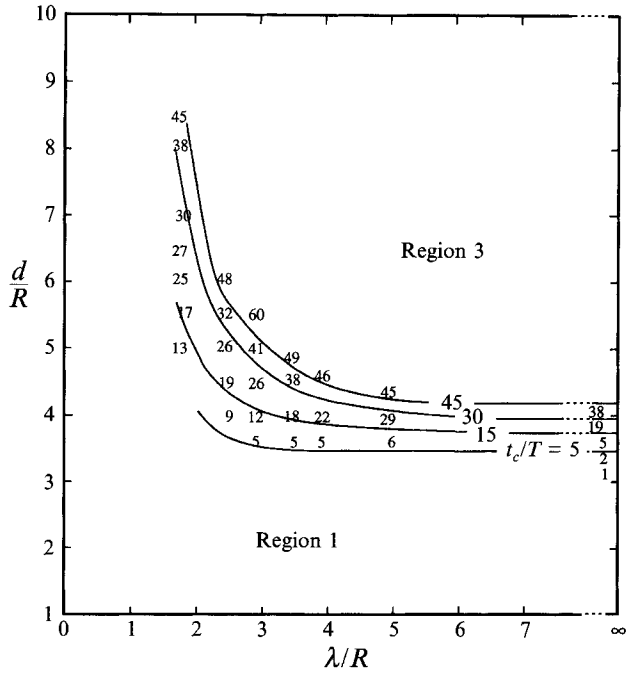

FIGURE 9. Merger time t_c/T as a function of d/R and of the equivalent shape factor λ/R for the barotropic simulations with $A_4^* = 1 \times 10^{-4}$. In Region 1, merging occurs rapidly on a convective timescale; in Region 3, viscous merging eventually occurs on a much longer viscous timescale. The isocurves for $t_c/T = 5$, 15, 30, 45 are shown.

distinction between relative and potential vorticity has no further significance. In other words, for the upper layer which is of interest here, one is reduced to studying the interaction between two vortices, the initial shape of which is given by

$$\omega_{10}^k = \sum_{k=1,2} R_a^k - \tfrac{1}{2}\lambda^{-2}\psi_{10}^k,$$

with ψ_{10}^k given as the solution of the system

$$\nabla^2\psi_{10}^k = R_a^k.$$

Since stratification is no longer dynamically present, λ/R is no longer a measure of the Rossby radius but becomes simply a factor that governs the initial vortex shape. Varying λ changes the initial shape of the vortices, just as the initial potential vorticity profiles of the vortices were changing with stratification in the RVI case. In particular, the characteristic 'skirt' shape of the vortices becomes increasingly pronounced as λ/R decreases. (If the second layer is considered on its own, the problem reduces to the purely two-dimensional interaction of vortices defined as $\omega_{20}^k = \frac{1}{2}\lambda^{-2}\psi_{10}^k$.)

It is now possible to study the barotropic merging problem for the upper layer with different initial vortex shapes as λ/R varies. The results are presented in figure 9 which, using the same scales as before, shows merger times t_c/T as a function of d/R and λ/R (which is now a shape factor) for each simulation. It may be observed that, for each particular value of d/R, t_c/T decreases as λ/R decreases. It may therefore be concluded that the more pronounced the 'skirt' shape is, the greater the tendency for vortices to merge. This is not really surprising if one considers that the influence of the vortices on each other increases as the vorticity profile extends from their core.

The interesting point is that the isocurves for $t_c/R = 5, 15, 30, 45$, in figures 9 and 5 coincide almost perfectly for $3.2 < \lambda/R < \infty$ and, in both cases, the tendency to merge continues to increase strongly with decreasing λ/R. This is even more pronounced in the RVI case (figure 5).

This means that, in the RVI case, the pure effect of the shape of the upper-layer potential vortices is likely to be the principal reason for the increased tendency to merge when λ/R decreases from ∞ to about 3. Or, in other words, no coupling effect between the layers is really active in this range (except, maybe for $3.0 < \lambda/R < 3.2$, where the RVI tendency to merge is even greater than in the pure barotropic case). The increased tendency to merge for $\lambda/R > 3$ should therefore be mainly a consequence of (passive) shape adjustment in the presence of stratification, but no significant baroclinic dynamics is subsequently required.

3.2. *Heton interaction*

Let us now consider the two-layer system in the RVI for small values of λ/R. In the expression of the RVI initial potential vorticity (8), the stretching term $\lambda^{-2}\psi_{10}$ is now relatively large. For each vortex initiated in the upper layer, there is a corresponding vortex of opposite sign in the lower layer associated with this stretching term (figure 4*a*). For small λ/R, the lower-layer vortices become appreciable compared with the upper-layer vortices (the ratio of upper to lower vortex amplitudes is, however, always > 1) and their dynamical effect can no longer be neglected.

For small λ/R, the RVI situation becomes equivalent to the initialization in potential vorticity of two vortices in the upper layer and two vortices of opposite sign in the lower layer. This is analogous to an initial configuration of two hetons as described by Hogg & Stommel (1985*a*). Hogg & Stommel originally defined a heton as a pair of opposite-sign point vortices in opposite layers. In the present case, the major differences are that the vortices have finite cores instead of being point vortices and that their cores have a specific shape defined by (8).

Hogg & Stommel (1985*a*) studied the interactions between point-vortex hetons. They assumed, as in the present study, that the flow satisfies the quasi-geostrophic potential vorticity equations. By considering the invariants of the equations describing the motion of the vortices, they found that the ratio $d/\lambda = 1.43$ (where d is the initial distance between the two hetons) was critical for the behaviour of the vortices. When $d/\lambda < 1.43$, the interaction between vortices in the same layer is stronger than the coupling through the interface. The two positive vortices in one layer and the two negative vortices in the other layer simply circle around their mutual centre of vorticity, counterclockwise and clockwise respectively as shown schematically in figure 10(*a*). When $d/\lambda > 1.43$, each heton initially splits the other; but then, as stratification is relatively weak, the interaction across the interface between the two vortices of each heton becomes dominant and the two tilted hetons self-propel in opposite directions. This behaviour is shown in figure 10(*b*) for the case of hetons composed of opposite-sign vortices of equal intensity. When the intensity of the negative vortices is smaller than the intensity of the positive vortices the divergence motion takes a curved path as shown in figure 10(*c*).

In order to generalize the Hogg & Stommel point-vortex computations, we investigated the interactions between two equal finite-core hetons in which each vortex was of the Rankine type $\pm R_a^k$, as defined above. The detailed results of this particular study are presented in Valcke & Verron (1993). The merger times t_c/T, defining three regions of exactly the same nature as the regions defined for the RVI case, are shown in figure 11 as a function of d/R and λ/R. For large λ/R, the interaction between the

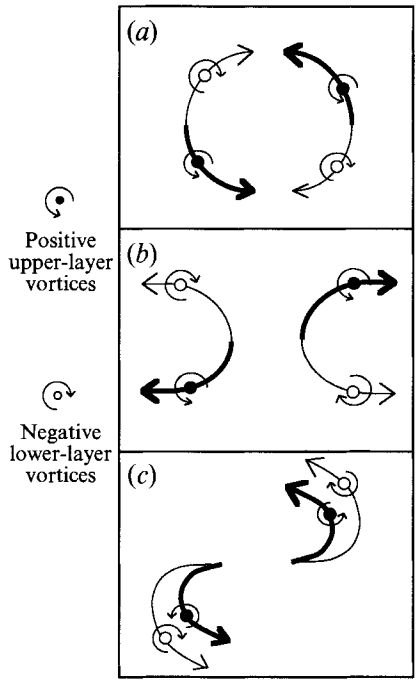

FIGURE 10. Trajectories of the vortices resulting from the interaction between point-vortex hetons: (*a*) for $d/\lambda < 1.43$; (*b*) for $d/\lambda > 1.43$, case of hetons made up of opposite-sign vortices of equal intensity; (*c*) as in (*b*) except that the intensity of the lower-layer vortices is smaller than the intensity of the upper-layer vortices.

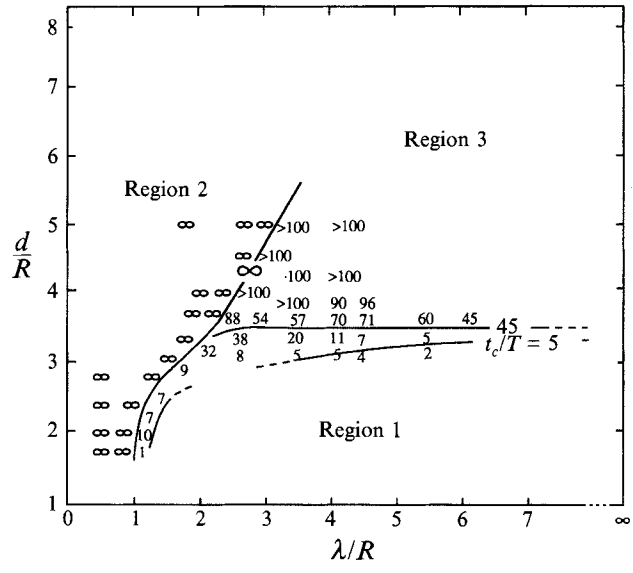

FIGURE 11. Merger time t_c/T as a function of d/R and λ/R for finite-core hetons with $A_4^* = 2 \times 10^{-5}$. The characteristics of the regions are as in figure 5. The isocurves for $t_c/T = 5$, 45 and ∞ are shown.

vortices is qualitatively the same as if the layers were uncoupled. In Region 1, the vortices merge on a convective timescale, while in Region 3 they do not. In the latter region, viscous merging eventually occurs on a viscous timescale. In Region 2, behaviour is analogous to the point-vortex behaviour for $d/\lambda > 1.43$. Initially, each

heton is split by the other, but, once the two hetons are tilted, they begin to self-propel in opposite directions and diverge. This type of interaction is specific to hetons when stratification is relatively weak, and we will refer to it as the 'heton effect'. The most interesting conclusion concerns Region 2: for $\lambda/R < 2$ approximately, the divergence motion is strong enough to increase the distance between the same-layer vortices even when d/R is such that they would normally undergo convective merging. The tendency to merge is therefore very much countered.

These results lead us to conclude that the divergence behaviour typical of Region 2 in the RVI case could be explained by the heton effect. For a weak stratification, the vortices created in the lower layer are relatively intense and their dynamical effect is to make the upper-layer vortices diverge, thereby inhibiting merging. After the initial splitting of the two vortices of each heton, coupling through the interface of these two vortices makes the hetons travel in opposite directions. As the lower-layer vortices are always less intense than the upper-layer vortices, the movement should be curved. This is indeed the case, as shown in figure 6(*a*): the lower vortices are dragged along by the stronger upper vortices in a cyclonic curved motion and the effect of coupling between the opposite-layer vortices is to make the same-layer vortices diverge from each other.

These considerations lead to the general conclusion that, as far as merging is concerned, the RVI behaviour, and in particular the increased tendency to merge for $1.5 < \lambda/R < 3$, is the result of two competing effects: one of *attraction*, resulting from a pure barotropic shape effect which tends to promote merging as λ/R decrease because of the growth of the vorticity 'skirt', and one of *repulsion*, caused by a heton-specific type of baroclinic interaction which, in a weakly stratified regime, tends to make the same-layer vortices diverge from each other, a phenomenon which becomes more intense as λ/R decreases. The peak area in the curves is the result of these competing effects.

3.3. *Consequences for the other types of initialization*

In the PVI case, the shape of the potential vorticity of the upper- and lower-layer vortices is determined initially by equations (7*a*) and (7*b*) and is independent of the stratification. Consequently, it is clear that in the PVI case, neither the shape nor the hetonic type of interaction should influence merging. It is therefore not surprising that, in the PVI case, merging is insensitive to stratification as discussed above.

In the MVI case (equations (9)), no hetonic type of interaction can be involved as the potential vorticity of the bottom layer is uniform and independent of stratification. The particular merging behaviour should therefore be entirely related to the shape of the potential vorticity of the upper-layer vortices. We have already noted that the 'skirt' shape of the potential vorticity profile becomes more pronounced as λ/R decreases from ∞ to $\lambda/R > 1$ (figure 7*a*). But, for small values of λ/R, the 'skirt' then becomes rapidly restricted to a region close to the core of the vortex. This change in shape is well illustrated in figure 7(*b*), which focuses on this 'reverse' skirt effect, apparent for the smallest λ/R. As we associated a more developed 'skirt' with a greater tendency to merge, the merging behaviour in the MVI case is compatible with this change in the skirt. As illustrated in figure 8, the tendency to merge increases progressively as λ/R decreases from ∞ to ≈ 1, but it then decreases suddenly as the 'skirt' itself diminishes.

The 'reduced gravity' situation is also interesting because it should exhibit only one side of the balance, namely the shape effect. No baroclinic counter effect of the hetonic type is present to balance the exponentionally increasing tendency to merge as λ/R decreases. Preliminary exploration of this case, as mentioned in §2.5, confirms this view

entirely. However, this cannot be strictly true for the limit $\lambda/R = 0$, since in this case taking the limit $H_2 \to \infty$ is no longer valid.

4. Real vortices and modelled vortices

Continuous stratification and ageostrophic effects make the real world rather different from the schematized eddies described in the previous sections. From §2, it is now clear that the vertical flow structure as well as details of the initial vortex profiles are of crucial importance to baroclinic vortex merger. In realistic situations (either geophysical or experimental) it should not be general that potential vorticity profiles will look like Rankine profiles. In fact, McWilliams (1990) has shown in numerical simulations of decaying geostrophic turbulence that vorticity variation is close to a Gaussian curve. However, Waugh (1992) argues that the merging of vortices with non-uniform vorticity in fact produces a vortex with sharper edges, and that this characteristic is even enhanced by the stripping resulting from interaction with surrounding vortices. On the other hand, specific numerical computations (Melander *et al.* 1988) have shown that the details of the very core of the vortex are, unlike the 'skirt'-shaped far field, relatively unimportant with regard to merging stability.

However, as stated previously, the fundamental issue should lie in the fact that eddies have a signature in potential vorticity throughout the whole water column. Both PVI and RVI modes of initialization are specific in some way. RVI assumes no initial motion within the bottom layer, while PVI assumes uniform potential vorticity in the deep flow. As can be seen in the theoretical equations, the relevant dynamical quantity is the potential vorticity. A relevant question now is whether 'real' eddies have any signature in potential vorticity all along the vertical or only at the surface (for example, only above the ocean thermocline).

4.1. *Oceanic vortices*

Relatively little is known about the detailed structure of eddies in the ocean. There is no doubt that these eddies have horizontal and vertical structures which are much more complicated than the simple representation discussed above. Moreover, they evolve within a complex dynamical environment.

In 1985, Arhan & Colin de Verdière presented a detailed analysis of field measurements taken during the Tourbillon Experiment in a region of the North East Atlantic. They were able, in particular, to carefully analyse the dynamical properties of an eddy. An interesting by-product of their study is the mapping of the relative and potential vorticity fields over the area. The relative vorticity of the eddy observed was of the same sign throughout the whole water column but was clearly intensified above the main pycnocline (850 m). The eddy potential vorticity seemed to be confined to the upper 1000 m. Horizontally, both relative and potential vorticities were intensified within the eddy core. Based on their findings, one is tempted to suggest that the eddy observed corresponds to a PVI situation in which the initial upper-layer potential vorticity profile exhibits variable spreading about the Rankine one.

The Gulf Stream rings are a particular case of long-lived vortices which has received considerable attention (see Joyce 1991 or Olson 1991 for a review). Olson (1980) gives a detailed analysis of the density, velocity, vorticity and energy distribution in the Gulf Stream cyclonic ring, designated Bob, observed in the 1977 Cyclonic Ring Experiment. The ring can be clearly identified by an anomaly in potential density and potential vorticity in the area between the surface and about 1500 m. The velocity field is also clearly stronger above 1500 m but the interesting point here is that the velocity field

shows a reversal in sign below 1000 db. This reversal in sign is also present below another ring, referred to as Al, described in the same paper. The author suggests that this could be a common feature in Gulf Stream cyclonic rings. This opposite-sign velocity in the bottom reminds one of the hetonic configuration associated with the RVI. Horizontally, the ring presents a solid-body-rotating core surrounded by a maximum in velocity, relative vertical vorticity and potential vorticity.

It is also interesting to note here that the idea of vortices characterized by an alteration of the lower-layer potential vorticity is not restricted to our RVI simulations but has already been proposed in the literature. Hogg & Stommel (1985*b*) use their 'heton' model to describe a pool of warm or cold water (such as a worm or cold Gulf Stream ring), and its properties of potential energy release through baroclinic instability and horizontal heat transport. Their two-layer model assumes that the potential vorticity of the bottom layer is of opposite-sign compared with the potential vorticity of the upper layer, thus agreeing with the RVI scheme.

From the above two oceanic examples, the impression is that it is difficult to reach a firm conclusion with regard to the relevant 'initialization' for each particular eddy. In addition, it is likely that several physical mechanisms involved in the production of eddies do not conserve potential vorticity. The Rankine representations of relative or potential vorticity confined in the upper layer seem to be overly simplistic, not only in the horizontal structure but also in the vertical structure where characteristics of the two types of initialization might be encountered.

4.2. *Experimental vortices*

Other types of 'real' eddies are clearly those produced in the laboratory as in the experiments by Griffiths & Hopfinger, the aim of which was to represent interactions between a pair of eddies using a two-layered stratified model.

These experiments were conducted in a rotating circular tank where a two-layer stratification was created with two layers of equal thickness but unequal density. Two like-sign vortices were initiated by the localized injection (resulting in anticyclones) or suction (cyclones) of fluid in the upper layer of the flow. Vortex interaction and merging conditions were studied for different configurations in a range of parameters corresponding approximately to $0 < \lambda/R < 3$. They found that the stratification strongly affects merging.

At first sight, there is a striking similarity, between the laboratory and the present RVI results, in the way stratification influences the merging tendency for the range of common λ/R values. Other aspects are more difficult to reconcile. In particular, the initial state of no motion for the bottom flow, as assumed by the RVI model, does not appear to be a realistic description of the experiments. Indeed, motion is present in the bottom layer as can be seen from the experimental velocity profiles. In fact, there is a greater correspondence between these ones and the PVI velocity profiles. The MVI situation introduced in §2.4 may seem to be the closer to the experiments conditions (see also Verron & Hopfinger 1991). First, in the MVI case, there is no anomaly of the potential vorticity in the bottom layer. (We recall that Griffiths & Hopfinger assumed that this was the case in their experiments). Second, as in the experiments, the bottom layer is not at rest. And third, the merging tendency is also influenced by the stratification (see figure 8).

Another important point pertains to the flow behaviour at small values of λ/R. In the RVI situation, baroclinic instability is encountered for small λ/R. In the PVI situation, as in the experiments, baroclinic instability is not observed. This is also the case in the MVI, since, with decreasing λ/R, the vertical shear becomes increasingly

smaller as does the baroclinic velocity field. In any case, the limiting situation $\lambda/R = 0$ cannot strictly be encountered because initial conditions are inconsistent with the barotropic situation corresponding to $\lambda/R = 0$.

Our numerical code was also used to conduct preliminary explorations of some of the various specific attributes of the experimental investigations that were not considered in the models such as lateral diffusion, bottom Ekman layer influence and spurious differential rotation in the layers. None of these investigations, however, provided clear conclusive results. The effect of linear bottom friction was also found to be relatively unimportant. Other possibilities, such as more complex interfacial dynamics, cannot easily be accounted for in the framework of quasi-geostrophy and were not investigated further.

The main point emerging from the laboratory investigations is that experimental merging is significantly affected by stratification. However, from the analysis made here, it is clear that a precise justification for this phenomenon and an accurate model for the horizontal and the vertical vorticity structure of the eddies in the experiment is yet to be found. At the moment, there is some doubt as to whether the assumption made by Griffiths & Hopfinger that the potential vorticity is uniform and constant in the bottom flow during vortex initialization is entirely satisfied. Some alterations of the constant potential vorticity field may occur, owing to some form of interfacial friction for example, resulting in a potential vorticity signature in both layers for the experimental eddies.

5. Summary

We have investigated numerically the interaction of a pair of equal eddies in a two-layer stratified fluid in order to assess the role that stratification could play in the merging process. The cases considered are those of vortices defined in relative or potential vorticity in the upper layer. By changing the mode of initialization used, it was possible to obtain several situations in which to examine the influence of stratification on the merging process.

In particular, initial conditions in which simple relative vorticity distributions are specified in each layer (RVI case) lead to merging conditions which are strongly dependent on the original eddy scales. It is found that in the range of stratification corresponding to λ/R between 1.5 and 3 approximately, merging is considerably favoured and occurs at convective timescales even when the initial distance between the eddies is large. For smaller λ/R, on the other hand, merging is strongly inhibited. In contrast, if simple initial distributions of potential vorticity are specified (PVI case), the vortices show no sign of being influenced by the stratification. The critical point here appears to be whether or not the initial eddies have a deep flow signature in terms of potential vorticity. Since the potential vorticity in the PVI case is specified to be constant everywhere in the lower layer, this should be a singular situation. But, the potential vorticity resulting from assuming no motion in the bottom layer in the RVI case is also in a way singular. These results should encourage further investigations of the influence of the initial conditions and the detailed depth-dependent structure on the dynamics of eddy–eddy interactions.

It was demonstrated that the behaviour observed in the RVI case with regard to merging may be understood as the result of the competing effects of a 'baroclinic heton-like' tendency of eddies to repel each other and a 'barotropic shape' tendency for them to attract each other. The horizontal scales of the so-called oceanic mesoscale eddies fall within the range of scales where these competing effects would be intense.

However, concerning the vertical structure, it does not appear easy to obtain relevant information from observations of some ocean eddies to determine whether they belong to a particular initial model type. Observations by Olson (1980) of Gulf Stream rings support the RVI scenario, but it is not so clear in the observations by Arhan & Colin de Verdière (1985) that any anomaly of potential vorticity is present in the deep flows for the Tourbillon experiment. The laboratory experiments by Griffiths & Hopfinger (1987) exhibit merging which is qualitatively similar to that revealed by our RVI results, but, as yet, it is not possible to determine with any certainty the origin of the likely potential vorticity perturbation in the bottom layer.

We are indebted to E. J. Hopfinger and J. C. McWilliams for their participation in fruitful discussions. We much appreciated comments on this paper by L. Polvani. Referees are also acknowledged for the pertinent remarks. Calculations were made using the numerical facilities of the Centre de Calcul Vectoriel pour la Recherche in Palaiseau.

REFERENCES

ARHAN, M. & COLIN DE VERDIÈRE, A. 1985 Dynamics of eddy motion in the eastern North-Atlantic. *J. Phys. Oceanogr.* **15**, 153–170.

BASDEVANT, C., LEGRAS, B., SADOURNY, R. & BELAND, M. 1981 A study of barotropic model flows: intermittency, waves and predictability. *J. Atmos Sci.* **38**, 2305–2326.

BROWN, G. L. & ROSHKO, A. 1974 On density effects and large structures in turbulent mixing layers. *J. Fluid Mech.* **64**, 775–816.

CARNEVALE, G. F., CAVAZZA, P., ORLANDI, P. & PURINI, R. 1991 An explanation for anomalous vortex merger in rotating-tank experiments. *Phys. Fluids* A **3**, 1411–1415.

DRITSCHEL, D. G. & WAUGH, D. W. 1992 Quantification of the inelastic interaction of unequal vortices in two-dimensional vortex dynamics. *Phys. Fluids* A **4**, 1737–1744.

GORDON, A. L. & HAXBY, W. F. 1990 Agulhas eddies invade the South Atlantic – evidence from Geosat altimeter and shipboard conductivity temperature depth survey, *J. Geophys. Res.* **95**, 3117–3125.

GRIFFITHS, R. W. & HOPFINGER, E. J. 1987 Coalescing of geostrophic vortices. *J. Fluid Mech.* **178**, 73–97.

GRYANIK, V. M. 1983 Dynamics of singular geostrophic vortices in a two-level model of the atmosphere (or ocean). *Izv. Akad. Nauk. SSSR Atmos. Oceanic Phys.* **19**, 171–179.

HOGG, N. & STOMMEL, H. 1985*a* The heton, an elementary interaction between discrete baroclinic geostrophic vortices and its implications concerning eddy heat-flow. *Proc. R. Soc. Lond.* A **397**, 1–20.

HOGG, N. & STOMMEL, H. 1985*b* Hetonic explosion: the breakup and spread of warm water pools as explained by baroclinic point vortices. *J. Atmos Sci.* **42**, 1465–1479.

HOLLAND, W. R. 1978 The role of mesoscale eddies in the general circulation of the ocean – Numerical experiment using a wind driven quasi-geostrophic model. *J. Phys. Ocean* **8**, 363–392.

HOPFINGER, E. J. & HEIJST, G. J. F. VAN 1994 Vortices in rotating fluids. *Ann. Rev. Fluid Mech.* **25**, 241–289.

JOYCE, T. M. 1991 Review of US contributions to warm-core rings. *Rev. Geophys. Suppl.*, 610–616.

MELANDER, M. V., ZABUSKY, N. J. & MCWILLIAMS, J. C. 1988 Symmetric vortex merger in two dimensions: causes and conditions. *J. Fluid Mech.* **195**, 303–340.

MCWILLIAMS, J. C. 1984 The emergence of isolated coherent vortices in turbulent flow. *J. Fluid Mech.* **146**, 21–43.

MCWILLIAMS, J. C. 1989 Statistical properties of decaying geostrophic turbulence. *J. Fluid Mech.* **198**, 199–230.

MCWILLIAMS, J. C. 1990 The vortices of geostrophic turbulence. *J. Fluid Mech.* **219**, 387–404.

OLSON, D. B. 1980 The physical oceanography of two rings observed by the cyclonic ring experiment. Part II: Dynamics. *J. Phys. Oceanogr* **10**, 514–528.

OLSON, D. B. 1991 Rings in the ocean. *Ann. Rev. Earth Planet. Sci.* **19**, 283–311.

OVERMAN, E. A. & ZABUSKY, N. J. 1982 Evolution and merger of isolated vortex structures. *Phys. Fluids* **25**, 1297–1305.

PEDLOSKY, J. 1979 *Geophysical Fluid Dynamics.* Springer.

POLVANI, L. M. 1991 Two-layer geostrophic vortex dynamics. Part 2. Alignment and two-layer V-states. *J. Fluid Mech.* **225**, 241–270.

POLVANI, L. M., ZABUSKY, N. J. & FLIERL, G. R. 1989 Two-layer geostrophic vortex dynamics. Part 1. Upper layer V-states and merger. *J. Fluid Mech.* **105**, 215–242.

VALCKE, S. & VERRON, J, 1993 On interactions between two finite-core hetons. *Phys. Fluids* A **5**, 2058–2060.

VERRON, J. & HOPFINGER, E. J. 1991 The enigmatic merging conditions of two-layer baroclinic vortices. *C. R. Acad. Sci. Paris* **313** (II), 737–742.

VERRON, J., HOPFINGER, E. J. & MCWILLIAMS, J. C. 1990 Sensitivity to initial conditions in the merging of two-layer baroclinic vortices. *Phys. Fluids* A **2**, 886–889.

WAUGH, D. W. 1992 The efficiency of symmetric vortex merger. *Phys. Fluids* A **4**, 1745–1758.

WINANT, C. D. & BROWAND, F. K. 1974 Vortex pairing: the mechanism of turbulent mixing layer growth at moderate Reynolds number. *J. Fluid Mech.* **63**, 237–255.

ZABUSKY, N. J., HUGHES, M. H. & ROBERTS, K. V. 1979 Contour dynamics for the Euler equations in two dimensions. *J. Comput. Phys.* **30**, 96–106.